Accepted Manuscript

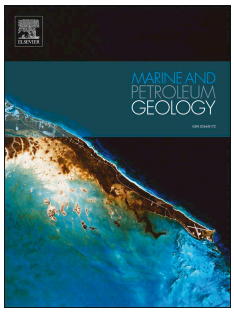

Laboratory characterization of the porosity and permeability of gas shales using the crushed shale method: Insights from experiments and numerical modelling

Quentin Fisher, Piroska Lorinczi, Carlos Grattoni, Konstantin Rybalcenko, Anthony J. Crook, Samuel Allshorn, Alan D. Burns, Ida Shafagh

PII: S0264-8172(17)30186-1

DOI: 10.1016/j.marpetgeo.2017.05.027

Reference: JMPG 2920

To appear in: *Marine and Petroleum Geology*

Received Date: 16 January 2017

Revised Date: 17 May 2017

Accepted Date: 18 May 2017

Please cite this article as: Fisher, Q., Lorinczi, P., Grattoni, C., Rybalcenko, K., Crook, A.J., Allshorn, S., Burns, A.D., Shafagh, I., Laboratory characterization of the porosity and permeability of gas shales using the crushed shale method: Insights from experiments and numerical modelling, *Marine and Petroleum Geology* (2017), doi: 10.1016/j.marpetgeo.2017.05.027.

Laboratory characterization of the porosity and permeability of gas shales using the crushed shale method: Insights from experiments and numerical modelling

Quentin Fisher[1], Piroska Lorinczi[1], Carlos Grattoni[1], Konstantin Rybalcenko[1], Anthony J. Crook[2], Samuel Allshorn[1], Alan D. Burns[1] and Ida Shafagh[3]

[1]*School of Earth and Environment, University of Leeds, Leeds, LS2 9JT, UK*

[2] *Three Cliffs Geomechanical Analysis Ltd, Roseleigh, Swansea, SA3 2EN, UK*

[3]*School of Civil Engineering, University of Leeds, Leeds, LS2 9JT, UK*

Abstract

Gas production from shale resource plays has transformed the USA energy market. Despite the knowledge gained from the analysis of large amounts of shale core, appraisal of shale gas resource plays requires a large number of wells to be drilled and tested. Ideally, core analysis results would provide an indication of both the gas filled porosity and permeability of shale resource plays, which could then be used to reduce the number of wells needed during appraisal. A combination of laboratory experiments, numerical modelling and a round-robin test have been conducted to assess the validity of the crushed shale method (CSM), which has been widely used in industry to assess the porosity and permeability of shale. The results suggest that the CSM can provide reasonably precise estimates of porosity measured at ambient stress if a standard sample cleaning method is adopted; although a reliable method to correct these values to subsurface conditions needs to be developed. The CSM does not, however, appear to provide useful information on shale permeability. A round-robin test shows that differences of up to four orders of magnitude in permeability were provided by different laboratories when analysing the same sample. These huge differences seem to occur due to a combination of errors in calculating permeabilities from pressure transients, differences in the way that permeability is calculated as well as uncertainties regarding the effective size of crushed shale particles. However, even if standardized, the CSM may not be particularly useful for characterizing the flow capacity of shale because it is insensitive to the presence of high permeability zones that would control flow in the subsurface.

Keywords: shale gas, permeability, porosity, crushed shale method, pressure transient analysis

Introduction

Shale gas production has revolutionized the energy market in the USA where production reached 40 bcf/d in 2015 and contributed around 50% of the total dry gas produced (IEA, 2015). By 2014, over 50,000 producing wells had been completed in the seven key shale gas plays, Barnett, Haynesville, Woodford, Fayetteville, Marcellus, Eagle Ford, and Bakken (Hughes, 2015). Exploration and appraisal of shale gas resource plays is now active in many other parts of the world including: Australia, Argentina, China, India, Mexico, Poland, Romania and the UK. Appraisal of shale gas resource plays remains difficult and expensive despite the large number of wells that have been drilled, cored and tested. For example, Haskett (2014) suggested that over ten pilot wells may be needed to have 90% confidence that the results are representative of the shale gas play. Also, up to 100 wells may be needed before optimal production efficiency has been reached and production costs minimized (Haskett, 2014).

Appraisal of shale gas resource plays differs significantly from that of conventional reservoirs. In particular, appraisal of conventional reservoirs often involves drilling, coring and testing a small number of wells and then building geological and simulation models based on core analysis data to predict the volume of petroleum present and future production rates as well as to optimize production strategies. Appraisal of shale gas resource plays involves the drilling and testing of far more pilot wells with less emphasis on core analysis and little or no emphasis on production simulation modelling.

The reduced emphasis on core analysis and production simulation modelling in shale gas resource plays is a response to several realities. First, there remains a large uncertainty regarding how gas flows from the shale matrix to hydraulic fractures. For example, the role of natural fractures, sedimentary lamina with higher permeability, and the presence of intragranular vs. organic matter porosity in controlling gas storage and flow rates are still widely debated (e.g. Schieber, 2010; Curtis et al., 2012). Second, shale gas resource plays are heterogeneous in terms of their sedimentology, gas distribution, fracture content and stress magnitude/orientation so many wells are needed to estimate average performance. Third, there are no well-established links between core analysis results and production rates. Indeed, despite a large number of core analysis measurements being conducted, there exists little consensus on how they can be used to estimate flow rates. Forth, industry-standard protocols for the analysis of shale core do not exist. Indeed, comparative studies, often referred to as round-robin tests, indicate laboratories provide very different

measurements of key properties, such as porosity and permeability (Passey et al., 2010; Dadmohammadi et al., 2016).

The current paper addresses key issues regarding the analysis of cores obtained from shale gas resource plays. In particular, it attempts to critically appraise the meaning of results from the laboratory method most commonly used by industry to assess the porosity and permeability of shale samples – namely the crushed shale method. In doing so, it attempts to identify causes of discrepancies between laboratories and provide recommendations for future core analysis. The paper begins by providing a review of the laboratory techniques that are commonly used to assess the porosity and permeability of core samples from shale gas resource plays. Results from numerical modelling and laboratory analysis are then used to provide some insight into the meaning of porosity and permeability data obtained from shales. The laboratory experiments conducted by the authors of this paper have been combined with a round-robin test in which the porosity and permeability of six shale samples have been analyzed by three of the leading companies providing shale analysis services to industry.

Laboratory characterization of the storage and flow capacity of gas shale

Porosity and permeability analysis of conventional reservoirs

To place the analysis of gas shale into context, the methods that are commonly used to measure storage and flow capacity of conventional reservoirs are briefly described. Porosity is the primary measure of the total storage capacity of gases and liquids in conventional petroleum reservoirs. Permeability is used as the main measure of the flow potential of conventional reservoirs. Porosity and permeability are usually measured on 1 or 1.5 inch diameter core plugs, which have been cleaned and dried to remove brine, hydrocarbons and drilling fluids.

The porosity of conventional reservoirs is defined as the pore volume divided by bulk volume. Pore volume is generally not measured directly. Instead, porosity is calculated from measurements of bulk, $\rho_{B,}$ and grain, ρ_G, density using:-

$$\emptyset = 1 - \frac{\rho_B}{\rho_G} \tag{1}$$

Mercury immersion has long-time been considered the gold standard for bulk density analysis although laser scanning is increasingly being used so as to reduce the use of toxic mercury. Grain density is usually determined using helium pycnometry. Bulk density is normally measured at ambient stress conditions so pore volume compressibility corrections need to be applied to extrapolate porosity measurements to *in situ* conditions.

Permeability of conventional petroleum reservoirs is generally measured using steady-state gas permeametry. In such tests, core plugs are placed in a core holder and confined at a pressure of ~500 psi. Gas flow is initiated through the sample until steady-state is achieved and then permeability, *k*, is calculated using an adaptation of Darcy's Law, which takes into account the variable gas density across the sample:-

$$k = \frac{QL\mu}{A(P_1^2 - P_2^2)} \quad (2)$$

where Q is flow rate, μ is viscosity, P_1 and P_2 are the upstream and downstream gas pressures at steady-state, A and L are the cross sectional area and length of the core.

Gas slippage enhances flow rates in low permeability sandstones so a Klinkenberg correction is often applied to the measurements to obtain what is often referred to as the absolute or liquid permeability, k_∞. The best practise is to measure the gas permeability at several different pressures and then calculate k_∞ by extrapolating plots of apparent permeability (i.e. the measured permeability value without a slip correction) against the reciprocal of the average pressure, P, to $1/P = 0$. Laboratory measurements of permeability of tight rocks are often very stress sensitive so an overburden correction is often applied to estimate *in situ* permeability values.

Laboratory analysis of shale samples

Laboratory analysis of the storage and flow capacity of shale samples is far more complex than for conventional reservoirs for both practical and theoretical reasons. The first practical difficulty is that it is generally far more difficult to obtain high quality core plugs from shale than it is for conventional reservoir rocks. This difficulty can be caused by shales delaminating as core plugs are taken or as a result of the damage that occurs during coring and core retrieval. The low permeability of shale means that gas pressure does not easily equilibrate via natural matrix or fracture porosity as the core is brought to the surface. In such cases, it expands to create microfractures along which it flows to reach pressure equilibrium (Zubizarreta et al., 2011, 2013; Ashena et al., 2016). The low permeability of shale samples means that core plugs are very difficult to clean. Also traditional porosity and permeability measurements are very time-consuming, which makes the results very susceptible to leaks from the experimental apparatus. The inability to obtain high quality core plugs also means that it is often very difficult to measure the pore volume compressibility of shale, which is needed to estimate porosity at *in situ* conditions.

There are several issues that impact the measurement of the storage capacity of shales, which are related to pore size and composition. For example, much of the pore-space in

shale is on the nm-scale so may be less accessible to methane than to helium. So the grain volume measured using helium could be lower than measured using methane. However, methane adsorption may lead to the swelling of organic matter, which would mean that pore volume could be overestimated when measured using helium compared to the natural situation where methane is present.

Measuring the gas flow capacity of shales has many of the same issues as for porosity but is also faced with the additional issue that unlike conventional gas reservoirs, where the principle flow mechanism is continuum (i.e. Darcy) flow, gas flow in shales may be dominated by other mechanisms such as slippage, transitional flow or Knudsen diffusion (Freeman et al., 2011). Gas flow mechanisms depend on the Knudsen number, which is the ratio of mean free path of the gas molecules to a characteristic length scale; the latter is generally assumed to be equivalent to the pore-size. The mean free path of gas molecules is strongly dependent on pressure-temperature conditions, which means that gas flow mechanisms in the laboratory may differ to those in the subsurface.

New laboratory methods and numerical models for measuring gas flow in shale have been developed that attempt to address some of these difficulties. Transient pressure techniques are often used to increase the speed of measuring permeability on core plugs. For example, Brace et al. (1968) developed the pulse decay permeametry, PDP, which is often used to measure shale permeability. The PDP test involves applying a pressure pulse to one end of the sample and recording the response in a downstream reference volume. The pressure transient is then used (i.e. inverted) to calculate permeability. Improvements in the model used to invert the pressure transient data have been developed by several groups (e.g. Lin, 1977; Hsieh et al. 1981; Neuzil et al. 1981; Dicker and Smits, 1988).

Numerical models have also been developed to allow the results from pressure transient tests to take into account gas flow mechanisms other than continuum flow (i.e. gas slippage and Knudsen diffusion) as well as gas adsorption on organic matter (e.g. Cui et al., 2009; Civan et al., 2011a,b). Linking these models to inversion algorithms provides the theoretical framework to obtain the key parameters that control gas flow in shale from the transient experiments. However, it has been argued that these models may contain too many unknowns, of which several are too closely correlated, to allow their use in the day-to-day analysis of shale (Lorinczi et al., 2014).

Although these developments go some way to increase the speed of sample analysis and take into account potentially important processes affecting gas flow in shale, they do not address other key issues such as the difficulty in obtaining and then cleaning undamaged shale core plugs. So a far more radical solution was proposed by workers at the Gas

Research Institute (Luffel and Guidry, 1992; Luffel et al., 1992; Luffel, 1993; Luffel et al., 1993) to address these issues. The method proposed, commonly referred to as the GRI or crushed shale method, CSM, involves conducting transient pressure experiments on crushed shale using an experimental set up similar to that illustrated in **Figure 1.** Crushed shale is placed into a sample chamber into which helium gas is expanded from a reference chamber at a known initial pressure. The pressure rapidly drops to a value dictated by the dead space in the sample cell, then it decays more slowly to a lower pressure as the gas moves into the pores within the crushed shale particles. Material balance is then used to calculate the grain volume and analytical or numerical methods are used to invert the pressure transient to calculate an apparent permeability. Bulk density is usually measured separately using mercury immersion. However, it has also been suggested that it is possible to extrapolate the pressure vs time, t, data to $t^{0.5} = 0$ and then apply material balance to calculate the bulk volume of the crushed shale (Luffel et al., 1992). The combination of grain volume and bulk volume can then be used to calculate porosity in a single measurement.

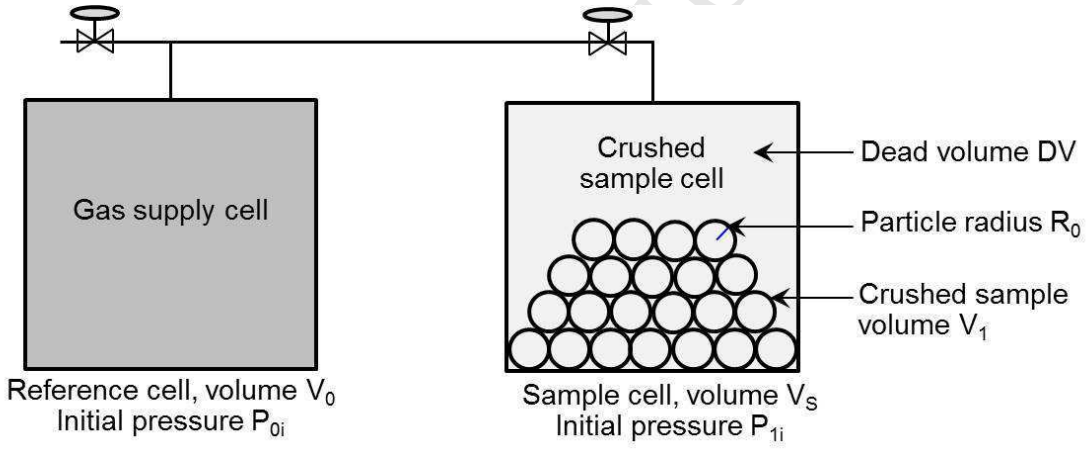

Figure 1 *Schematic diagram of a pressure pulsed-decay test of a crushed sample (after Profice et al., 2011).*

Luffel (1993) argued that the CSM had several advantages over the core plug based techniques including:-

- The high surface area to volume ratio of the crushed shale fragments means that the test can be conducted in a few minutes rather than the hours to days needed for the transient experiments on core plugs.
- The crushed shale particles are sufficiently small that they can be cleaned prior to analysis.
- The shale fragments along microfractures resulting in particles that are undamaged so the results could be treated as being true matrix properties.

These arguments have led to the CSM becoming widely used by the shale gas industry as the preferred method for measuring porosity and permeability. However, despite its

widespread use, many concerns have been raised regarding the validity of the CSM. For example, round-robin tests have shown that considerable differences in results are provided by different laboratories when the same shale sample was provided for analysis. In particular, Passey et al. (2010) report 100% differences in porosity and four orders of magnitude in permeability in the results provided by three leading service companies analysing the same samples. Several studies have suggested that the differences in porosity was due to the sample cleaning procedures used by the laboratories (Handwerger et al., 2011; Lalanne et al., 2014). In particular, one laboratory used the retort method to remove water and moveable hydrocarbons whereas the others used a solvent extraction technique followed by an extended period of drying (often in excess of a week) in a vacuum oven at 110^{o}C.

Causes for the differences in permeability results have not been as widely investigated, which is partly because service companies tend not to disclose the exact details of the sample analysis workflows, data inversion methods or even the raw pressure data collected during the experiments. Several theoretical arguments have, however, been raised about the validity of the CSM. A particularly important criticism is that interpretations of CSM results generally assume that Darcy flow is the main gas flow mechanism and ignore other gas flow mechanisms (Civan et al., 2015).

The models used to interpret CSM measurements range considerably in sophistication. The original work conducted by the Gas Research Institute used a simulation model to calculate permeability from pressure transients (Luffel et al., 1992). The simulation model assumed the shale fragments had a barrel shape, gas was not adsorbed to the constituents of the shale and that continuum flow was the dominant gas flow mechanism. Profice et al. (2011) provide an analytical solution for gas flowing into spherical shale particles, which also applies the Klinkenberg b-factor to take into account gas slippage. However, Profice et al. (2011) concluded that it was generally not possibly to accurately invert for both an absolute permeability and the Klinkenberg slip coefficient from a single measurement. Cui et al. (2009) also developed analytical solutions for gas flow into shale samples, which take into account gas adsorption on organic matter. Civan and Devegowda (2015) presented a sophisticated model for gas flow into shale particles, which takes account of gas adsorption as well as the key gas flow mechanisms. The model is solved numerically and combined with an inversion code that theoretically allows the key parameters controlling gas flow in shale to be inverted from CSM data. Mathur et al. (2016) described a sophisticated gas flow permeameter capable of conducting steady-state and transient permeability measurements on core plugs. The permeameter was used to conduct steady-state and transient gas permeabilities using helium and nitrogen at gas pressures ranging from 100 to 3200 psi

maintaining a net effective confining pressure of 3000 psi. The results from the experiments were within 30% of each other when a double slip correction was applied indicating that low pressure measurements are dominated by transitional flow. Dadmohammadi et al. (2016) described how the pressure step decay method could be used to make reproducible estimates of the permeability, porosity, pore volume compressibility and Klinkenberg b-value of ultralow permeability (~40 nD) pyrophyllite samples.

The effect of the shale particle size used in the CSM has been investigated by several authors (e.g. Cui et al., 2009; Profice et al., 2012; Tinni et al., 2012; Civan and Devegowda, 2015). In general, these studies have shown that the measured permeability increases as the size of the crushed shale fragments increases. For example, Tinni et al. (2012) found that permeability values can change by over two orders of magnitude when the size of the particle varies between 0.7mm and 7mm. Profice et al. (2012) suggested that a particle size should be used that is specifically selected to guarantee a reliable pressure decay recording. Using shale fragments that are too small results in a relaxation time that is too fast to be interpreted.

Another criticism of the CSM regards its inability to perform measurements at reservoir stress conditions or measure how permeability is likely to change during production (Heller et al., 2014). To tackle these flaws, Heller et al. (2014) carried out a series of laboratory experiments to investigate the effects of confining stress and pore pressure on permeability during production from gas shale reservoirs.

Experimental methods

A round-robin test has been conducted to better understand the reasons for the discrepancies between different laboratories using the CSM. Six 10-15 cm long, 10 cm diameter cores, here referred to as samples SH1-6, were cut perpendicular to bedding to obtain four identical subsamples. The samples were chosen because they appeared homogenous during visual inspection and from the analysis of CT scans generated from a medical-type CT scanner. Three of these subsamples were sent to different core analysis laboratories, here referred to as LabA, LabB and LabC, to have their porosity, permeability, grain density and bulk density analysed using the CSM. In addition, the laboratories were asked to take core plugs of the samples and measure permeability using the pulse-decay method. The forth subsample went through a very extensive sample analysis and characterization program at the University of Leeds. The analyses conducted at the various laboratories are described below.

Analysis conducted at the University of Leeds

The analysis conducted by the authors of this paper included a detailed sample characterization program as well as transient gas flow tests on both crushed shale and core plugs. The basic sample characterization program included:-

- Microstructural examination using scanning electron microscopy on samples polished using a broad ion beam polisher. These measurements were made on both polished thin sections made from both crushed and uncrushed core material.
- Mineralogical analysis using quantitative X-ray diffraction (QXTD)
- Major element analysis using X-ray fluorescence (XRF)
- Organic and inorganic carbon using an elemental analyser
- Surface area analysis using the BET method
- RockEval pyrolysis
- Hg-injection analysis was conducted on 1cm^3 shale samples using a Micromeritics Auto Pore IV porosimeter.
- Bulk density using mercury immersion
- Thermogravimetric analysis

A section of the core was then taken and crushed using an agate pestle and mortar. The crushed shale was sieved and the 20/35 mesh fraction (500 to 840 µm) retained for analysis using the CSM. This fraction was then divided into two subsamples. The first was treated as "as received" and analysed using the CSM. The second was weighed, oven dried at 110^{o}C for 7 days and then reweighed to determine the amount of liquid lost during drying. The samples were immediately placed in a desiccator prior to CSM analysis, which was conducted using a similar apparatus to that shown in **Figure 1**. The instrument used has reference and sample chamber volumes of 40.1 and 73.3 cm^3 respectively. Typical sample volumes of 25 to 35 cm^3 were used in the experiments. Helium gas at a pressure of 150-200 psig was expanded into the reference volume and allowed to reach temperature equilibrium before being expanded into sample chamber, which was typically at atmospheric pressure. Tests were conducted to assess whether varying the initial pressure between 150 and 200 psi significantly impacted the results but this proved not to be the case. Tests were also conducted to assess whether the results were improved by pre-flushing the cell with helium or placed under vacuum prior to analysis but no significant difference was identified. The pressure transient was recorded using a Mensor transducer at a rate of one measurement every 0.04s for around 2000s. Boyle's Law was used to determine the grain volume. Bulk volume was estimated from the weight of the sample and its bulk density. The latter was determined from mercury immersion measurements conducted on core plugs that were corrected for the weight loss that occurred during sample drying. The pressure transient was

used to calculate an apparent permeability using analytical and numerical methods described below (i.e. the permeability calculated was not Klinkenberg corrected).

Core plugs from the sample were also analysed using a pulse decay permeameter similar to that described by Jones (1997). The samples were confined at around 3000 psi and helium at a pressure of around 1000 psi was used as the permeant. The results from the experiment were inverted numerically using a dual porosity model in which a discrete fracture was incorporated into the model. The results from these experiments are included for completeness and will be described in more detail in a future publication.

Analysis conducted in LabA

Samples were analysed in this laboratory using virtually the same method as developed by GRI (Luffel et al., 1993). Each sample was weighed to ± 0.001 g and the bulk volume measured by Hg-immersion to ± 0.01 cm^3. A core plug was then drilled from each sample perpendicular to the lamination. The remaining sample was crushed with a mechanical rock crusher and sieved to obtain the 20/35 US mesh fraction. These steps were performed as quickly as possible to limit evaporation of fluids from the sample. The 20/35 fraction was then sealed in air tight vials and divided into two subsamples. Porosity and permeability of one subsample was measured using the GRI method. The second subsample was transferred to a Dean Stark apparatus and refluxed in toluene for 7 days. Fluid volumes were checked twice a day to ensure complete water extraction. The samples were then dried for at least a week at 110^oC and until weight stabilization (i.e. ± 0.001 g) was achieved. The samples were then transferred to a desiccator where they were kept until the porosity and permeability was measured using the same procedure as described by Luffel et al. (1993). The permeability measurements were made using helium gas at around 200 psig. Pressure measurements were made at 0.25 s intervals for a maximum of 2000 s. Oil and gas volumes were calculated from the results of the Dean Stark analysis assuming densities of 0.8 and 1.018 g/cm^3 respectively. The permeability of core plugs were measured using the PDP technique described by Jones (1997) at a helium pressure of 1000 psi and confining pressure of 5000 psi.

Analysis conducted in LabB

A core plug was then drilled from each sample perpendicular to the lamination. Bulk volume and bulk density were measured on the bulk sample as received although the exact method used was not disclosed by the laboratory. The sample remained after the core plug was taken was crushed and divided into two subsamples; no details were provided regarding the size of the shale fraction used. One subsample was treated as “as received” and analyzed using a proprietary version of the CSM. The numerical method used to calculate the

permeability from the pressure transient was not provided. The second subsample was used to measure the moveable oil, the total water content, the structural water and clay bound water using the retort method. The sample was then used to measure the dry grain density, porosity and permeability using a proprietary version of the CSM. No details were provided regarding how the samples were stored after drying. The core plug was analysed using a PDP technique but no information was provided regarding the instrument used or the algorithm used to calculate the permeability. Measurements on the core plug were made using a gas pressure of around 1000 psi and net confining pressures of 500, 1500, 3000 and 5000 psi.

Analysis conducted in LabC

Bulk volume and bulk density were measured on the bulk sample as received although the exact method used was not disclosed. A core plug was then drilled from each sample perpendicular to the lamination. The remaining sample was then crushed into particles of <1/8 in diameter before being divided into two subsamples. One subsample was treated as "as received" and the porosity and permeability measured using a propriety version of the CSM. The numerical method used to calculate the permeability from the pressure transient was not revealed. The second subsample was dried in a vacuum oven at 100^{o}C for an unspecified time and then analyzed using their propriety version of the CSM. No details were provided regarding how the samples were stored after drying. The core plugs were analysed using a PDP technique but no information was provided regarding the instrument used or the algorithm used to calculate the permeability.

Numerical modelling of gas flow in shale

A range of analytical and numerical models were used to both invert the pressure transient results obtained from the crushed shale experiments and also to explore key controls on the experiments; these are described below.

Analytical models

The analytical models presented by Profice et al. (2011) and Cui et al. (2009) were used to invert the pressure transient data obtained from the crushed shale experiments. The model of Profice et al. (2011) combined the mass conservation with the momentum conservation (Darcy-Klinkenberg) equations to give the following analytical solution:

$$P_0(t) = \left[\frac{3\gamma K}{3\delta K {R_0}^2 + {R_0}^3} + \frac{2}{R_0} \sum_m \frac{\gamma K exp\left(\frac{-{\xi_m}^2 K}{{R_0}^2} t \right) \sin(\xi_m)}{R_0[\delta K \xi_m \cos(\xi_m) + (R_0 + 2\delta K)\sin(\xi_m)]} + {P_{1i}}^2 \right]^{\frac{1}{2}}, \qquad (3)$$

where

$$\gamma = \delta {R_0}^2 \left({P_{0i}}^2 - {P_{1i}}^2 \right), \tag{4}$$

$$\delta = \frac{\mu (V_0 + DV)\beta_f}{S_T k} \tag{5}$$

and

$$K = \frac{k}{\phi \mu \beta_f} \tag{6}$$

The terms denoted by ξ_m are the roots of the equation:

$$\tan(\xi_m) = \frac{\xi_m}{1 + \frac{\delta K {\xi_m}^2}{R_0}} \tag{7}$$

Cui et al. (2009) developed an analytical method to calculate shale permeability from pressure transient obtained during the crushed shale experiment based on the one dimensional diffusion equation. The approach assumes that gas flow is controlled by Darcy's law and that the crushed shale fragments are spherical with a constant size. The method can also take into account gas sorption. Cui et al. (2009) suggest that the mass fraction, F_R, of gas in the reference cell and dead volume of the sample cell that is eventually incorporated into the shale can be calculated using:-

$$F_R = 1 - \frac{(K_c + 1)(\rho_{c0} - \rho)}{\rho_{c0} - \rho_0} \tag{8}$$

where for a non-absorbing gas K_c is the ratio of the dead volume in the experimental apparatus divided by the pore volume of the shale, V_b is the bulk volume of the shale, ρ_0 is the original gas densities in the reference cell, ρ is the gas density in the reference cell during the experiment and ρ_{c0} is the initial average gas density in the sample and reference cells given by:-

$$\rho_{c0} = \frac{\rho_{r0} V_r + \rho_0 (V_s - V_b)}{V_d} \tag{9}$$

where ρ_{r0} is the initial gas density in the reference cell. The slope, s_1, of the late-time behaviour of plots of ln(F_R) vs t can then be used to calculate permeability using the equation:-

$$k = \frac{R_a^2 \emptyset \mu c_g s_1}{\alpha_1^2} \quad (10)$$

where R_a is the radius of the shale fragments, μ is the gas viscosity, c_g is the gas compressibility, and α_1 is the first root of the equation:-

$$\tan \alpha = \frac{3\alpha}{3 + K_c \alpha^2} \quad (11)$$

In this analysis, late-time behaviour is defined being for dimensionless time, $t_D > 0.1$, where:-

$$t_D = \frac{t \mu \emptyset c_g}{k R_a^2} \quad (12)$$

Cui et al. (2009) also presented an early time solution for the CSM test. This was not used during the current study because the pressure measurements in the first few seconds of the gas entering the sample chamber were not stable.

Numerical models

Eclipse 100™ from Schlumberger was used to model gas flow into the shale particles. A double porosity permeability model with 10 x 10 x 42 grid blocks was constructed with each grid being a cube of 100µm length. The reference chamber was represented by 10 x 10 x 15 gridblocks. Two separate regions each of 6 x 6 x 8 grid blocks were placed in the centre of the remainder of the model to represent shale particles; these could be given the same or different poroperm properties for a single and double porosity model. The remainder of the cells within the model represented the dead volume in the sample chamber. The grid blocks representing the dead volume and reference chamber were assumed to have a permeability of 10 D and their porosity was adjusted so that the ratio of their pore volume to that of the total volume of shale was identical to the ratio of volumes of the shale to the space within the dead volume and reference volume. This model was then used to explore the controls on the GRI results and also to history match the experimental data. Enable™ from Emerson was used to history match the pressure transient data from the experiments. The software was set up to conduct 50 scoping runs in which the key unknowns, porosity and permeability, were randomly varied between the range estimated by the analyst. The software then employs a neighbourhood algorithm to identify the values which best fit the transient data using a further 50 refinement runs. The entire pressure transient after the measurements become stable (i.e. around 2s) is used in the history match procedure so this is equivalent to the late-time solution of Cui et al. (2009).

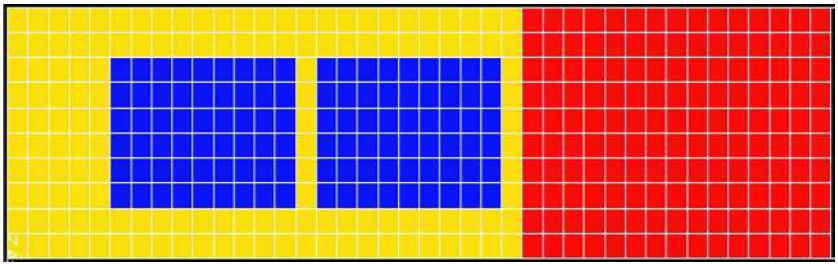

Figure 2 *Cross section of the grid used to model the crushed shale experiment. The red and yellow cells represent the reference volume and dead volume respectively whereas the blue cells represent the shale particles. The shale particles can be given the same or different poroperm properties for a single and double porosity model.*

Results

Bulk Density

The round-robin test showed that there was a reasonable agreement between the bulk density calculated by the four laboratories (**Figure 3**). In particular, standard deviation of bulk densities were 0.015g/cm^3, which is around 0.5%.

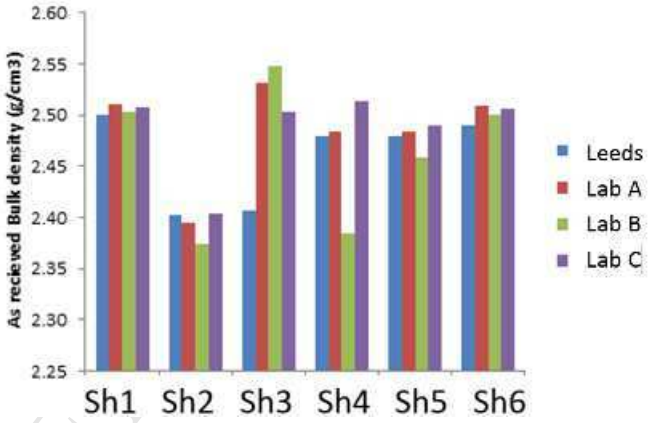

Figure 3 *Bulk density results from the round-robin experiment.*

Grain density

The round-robin test showed that there was a reasonable agreement between the grain density calculated by the four laboratories (**Figure 4**). In particular, standard deviation of grain densities was 0.02g/cm^3, which is around 0.8%. It should, however, be noted that LabB produced results that are around 0.05 g/cm^3 lower than the other laboratories. If data from LabB are removed the results from the other laboratories have a standard deviation of 0.013g/cm^3 or 0.5%.

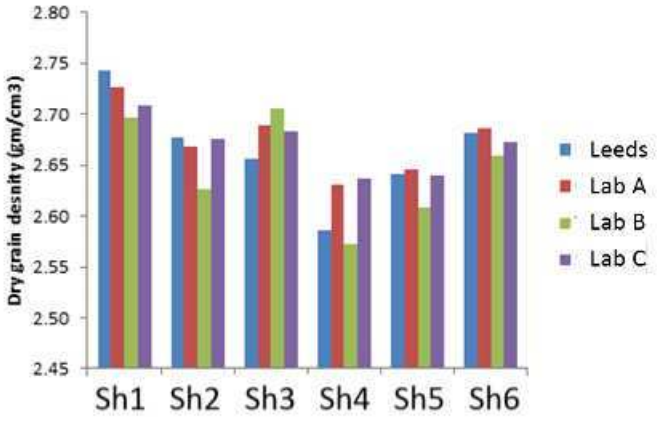

Figure 4 *Grain density results from the round robin experiment.*

Porosity

There is a reasonable agreement between the dry porosity obtained by the four laboratories. In particular, all porosity measurement agree within 0.9 p.u. with an average standard deviation of 0.67 p.u. (**Figure 5**). Porosity values produced by LabB are around 0.5 p.u. lower than the other three laboratories due to the differences in the grain density measurements. If LabB measurements are neglected the average standard deviation for the porosity measurements is <0.3 p.u.

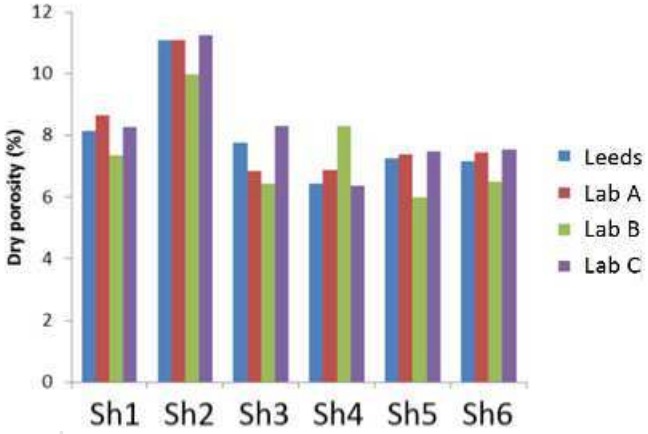

Figure 5 *Porosity results from the round robin experiment.*

Permeability

Crushed shale method

The permeability results obtained by the service companies using the CSM are provided in **Table 1**; the raw pressure data was not provided so it was not possible to conduct further analysis of the results. A far more detailed analysis could be conducted on the data collected by the authors. In all cases, the pressure in the reference volume rapidly falls and then starts to rise reaching a maximum at around 1s (**Figure 6**). The pressure then falls until it reaches the final equilibrium pressure, P_{eq}. The early time behaviour is always marked by an initial

rapid fall followed by a rise in pressure. It is tempting to assume that this early behaviour is caused by the cooling of the gas as a result of expansion. However, helium is not affected by the Joule-Thompson effect in this way at these pressure and temperature conditions. Instead, the instability of the early time data is possibly caused by the gas compressibility, flow through pipes and its expansion within the shale particles and the sample chamber. Multi-expansion tests were performed to assess whether these would result in increased pressure stability in this early time region but this proved not to be the case. Therefore, data collected during the first 2 seconds cannot be used to calculate permeability. Another feature of the results, which is important to the later discussion, is that P_{0i}, calculated by incorporating the initial pressures, cell and sample volumes into Boyles Law, is generally far higher than the initial pressure calculated by extrapolating P vs. $t^{0.5}$ to $t^{0.5} = 0$ (**Figure 7**). It appears that a certain proportion of helium enters the shale fragments along pathways that are more permeable than the remainder of the shale matrix.

The pressure data collected after two seconds were inverted for permeability using the analytical and numerical models described above; the results are summarized in **Table 2**. It was reasonably easy to estimate permeability using the model of Cui et al. (2009). However, it was noteworthy that the initial values of F_R ranged between 0.95 and 0.01. The low values indicate that a considerable proportion of the gas had entered the pore space of the shale fragments within the first two seconds after being expanded into the sample chamber. A second issue with the model of Cui was that in some cases the permeability calculated varied significantly depending on exactly which part of the $\ln(F_R)$ vs. time data were used.

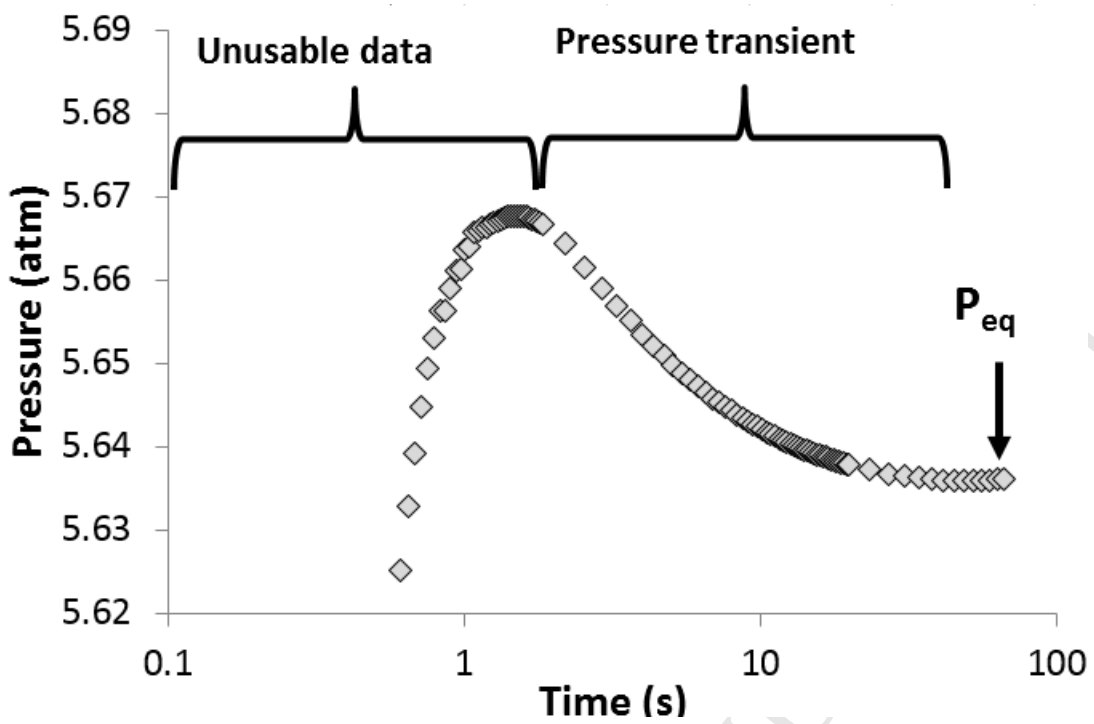

Figure 6 *Example of the pressure vs time behavior for the crushed shale tests.*

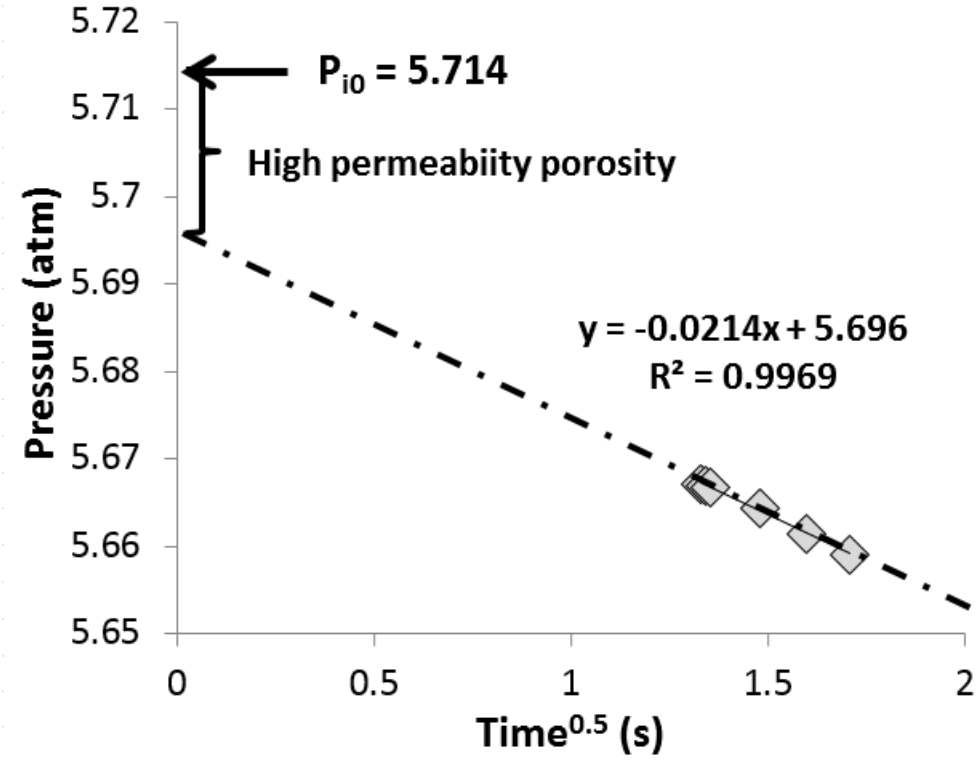

Figure 7 *Plot of pressure against square root of time. P_{0i} is the theoretical pressure of the gas in the dead volume before it has entered the pore space of the shale particles. The pressure calculated by extrapolating the pressure data to $t^{0.5} = 0$ is 5.696atm, which is signficantly lower than P_{0i}.*

It initially proved difficult to calculate permeability using the Profice model. In particular, the final pressure calculated by the Profice model was far higher than that calculated from the ideal gas law (Profice (a) in **Figure 8**). It was, however, noticed that for all experiments

incorporating a porosity value that was exactly double that calculated from the Ideal Gas Law into the model of Profice produced exactly the same final pressure as calculated from material balance (Profice (b) in **Figure 8**). The exact reason for this discrepancy has not been established but it appears most likely to be due to errors in the analytical solution provided by Profice et al. (2012). The best history match to the experimental data obtained using the model of Profice et al. (2012) was obtained by incorporating a value of P_{i0} calculated by extrapolating P vs $t^{0.5}$ to $t^{0.5} = 0$ into the model (Profice (c) in **Figure 8**). This is as opposed to P_{i0} calculated from the Ideal Gas Law using the initial volumes of the reference and sample volumes, the total volume of particles present as well as the initial pressures in the reference and sample volumes. Estimating P_{i0} by extrapolating P vs $t^{0.5}$ to $t^{0.5} = 0$ takes into account that shale particles appear to contain two pore systems; one which is accessed by the gas almost instantaneously and the true matrix porosity for which the model of Profice is used to estimate a permeability. In essence, this is the same as was achieved by the history match using the double porosity numerical model described below.

The Eclipse™-Enable™ model generally provided very poor history matches when a single porosity was used to represent the shale particles and the initial pressures, volumes, sample sizes and porosity calculated from material balance were used as input parameters for the model (Enable™ (a) in **Figure 9**). The double porosity-permeability model produced very good history matches, which were similar to the values obtained using the analytical models (Enable™ (b) in **Figure 9**). The history match was generally quite insensitive to the permeability used in the cells representing high permeability regions within the shale so long as they were higher than around 1mD. The model results were far more sensitive to the permeability value used to represent the shale matrix. Good history matches were also achieved by reducing the initial pressure and shale porosity so that the pore volume that was rapidly accessed by the helium was treated as part of the dead volume (Enable™ (c) in **Figure 9**).

Overall, the permeability results obtained in Leeds averaged over two orders of magnitude lower than provided by the service companies (**Figure 10**) and in some cases the difference exceeded four orders of magnitude. Correlations between the results from the different laboratories were in general non-existent (**Figure 11**). However, the permeabilities obtained using the analytical solutions and the double porosity numerical model were in good agreement.

Sample	LabA	LabB	LabC
SH1	330	530	34
SH2	440	160	250
SH3	110	46	1600

SH4	83	160	6
SH5	140	300	26
SH6	160	56	1500

Table 1 *Permeability data, in nD, provided by Labs A, B and C using the CSM.*

Sample	Cui	Profice	Eclipse™
SH1	1	1	4.8
SH2	4.1	4	7.9
SH3	0.042	0.056	0.03
SH4	0.8	1	0.66
SH5	0.27	0.3	0.09
SH6	0.07	0.1	0.07

Table 2 *Permeability results, in nD, determined in Leeds using the CSM. The data have been interpreted using two analytical models (Cui and Profice) as well as a numerical model (Eclipse™). The numerical results are from a dual porosity-permeability model but only the low permeability results are provided as the model was very insensitive to the high permeability results.*

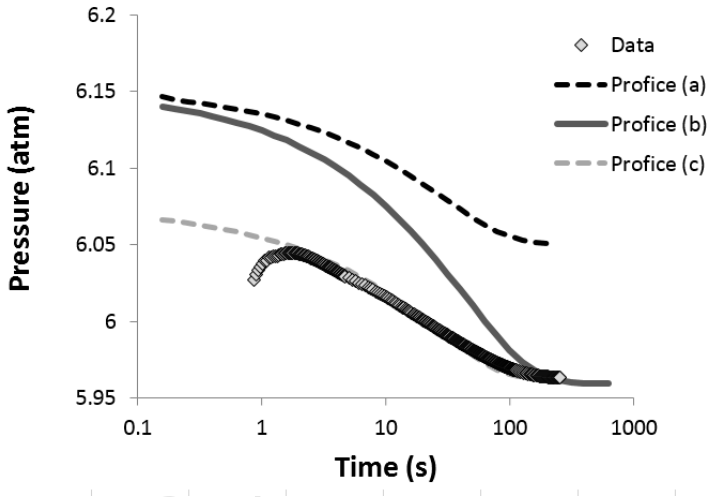

Figure 8 *Match between the experiment data and various model analytical models based on Profice et al. (2012); Profice (a) is the result obtained when using the porosity obtained by material balance and the initial pressure as input parameters; the permeability value used is the same as for the best fit analytical and simulation models. Profice (b) is similar to Profice (a) but double the porosity is entered into the model; Profice (c) was obtained by adjusting P_{i0} to that calculated by extrapolating the experimental P vs $t^{0.5}$ to $t^{0.5} = 0$ and then adjusting porosity and permeability to obtain a history match of the experimental data.*

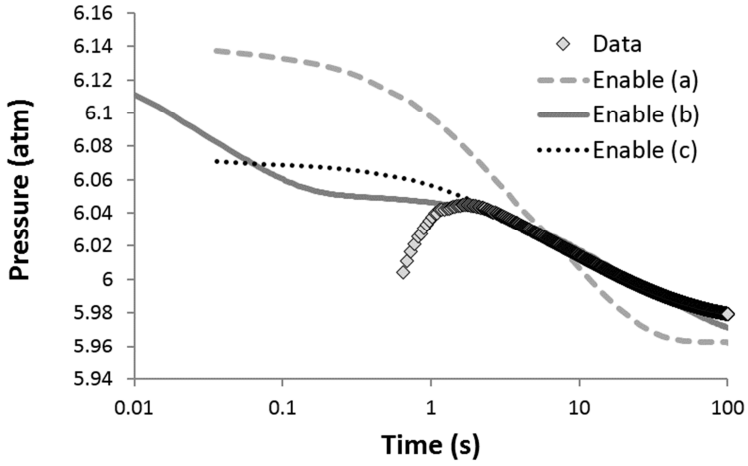

Figure 9 *History match using Eclipse™-Enable™ to model the experimental data. Enable™ (a) is a single porosity model that incorporated the porosity calculated from material balance and the initial pressure used in the experiment; the permeability was chosen to obtain the best fit of the experimental data. Enable™ (b) is a double porosity model in which the porosity and permeability two types of shale fragments were varied to achieve a history match. Enable™ (c) is a single porosity model in which the initial pressure and porosity are calculated so that the high permeability porosity is included as dead volume and the permeability altered to achieve a history match of the experimental data.*

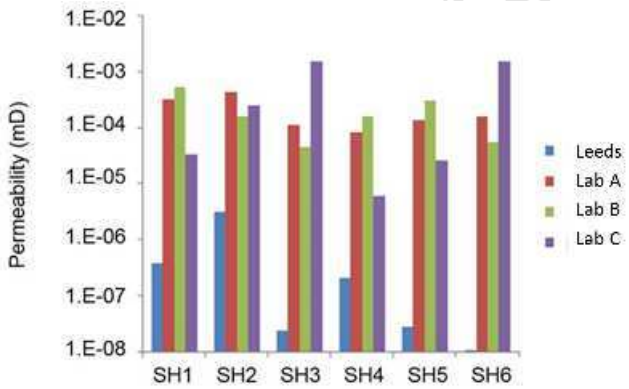

Figure 10 *Permeability results from the round-robin analysis of shale samples using the CSM; the Leeds permeability quoted here is thought to be that of the matrix (i.e. the low permeability in the dual permeability model).*

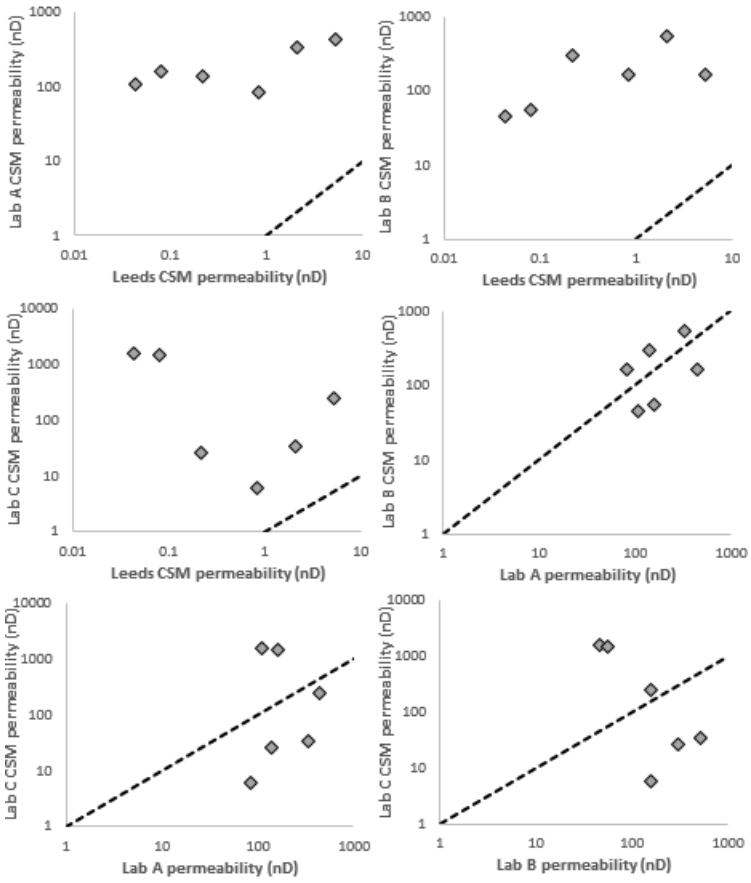

Figure 11 *Comparison of the results from the round-robin exercise for the crushed shale samples.*

Comparison with core plug measurements

For completeness, we have included results from pulse-decay tests conducted on shale core plugs (**Table 3**); the details of these tests will be discussed in more detail in a separate publication and these are merely presented here as a comparison with the crushed shale results. Overall, there was no clear correlation between the permeabilities obtained from crushed shale analysis and those measured on the core plugs (**Figure 12**). There are also no clear correlations between the permeabilities obtained using PDP between the different laboratories (**Figure 13**). In the case of results obtained from the service companies, it could be argued that the core plugs contained fractures and therefore the permeability values provided by the service companies did not represent those of the matrix. The PDP measurements conducted in Leeds were inverted for fracture and matrix permeability but there was still no correlation with the values obtained using the CSM.

Sample	Leeds	LabA	LabB
SH1	124	8370	120
SH2	287	240	680
SH3	70	360	493
SH4	0.44	5.8	294
SH5	0.44	2270	118

SH6	40	21	1180

Table 3 *Permeability data (in nD) obtained in Leeds and provided by two of the service companies; LabC did not manage to drill core plugs to make these measurements.*

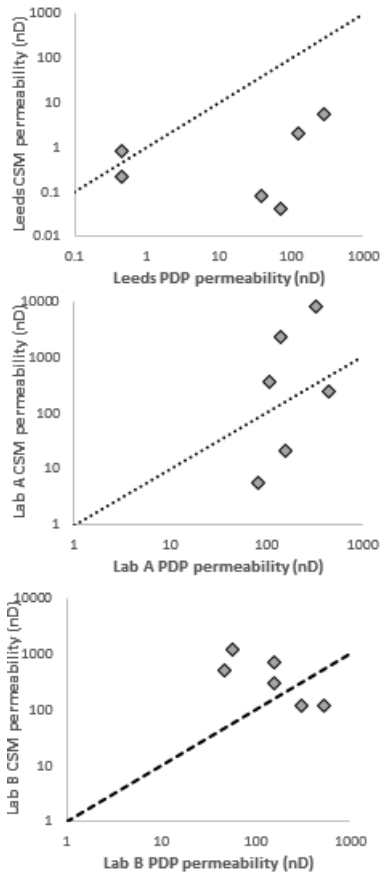

Figure 12 *Comparison of permeability values obtained from the crushed shale and core plug PDP technique.*

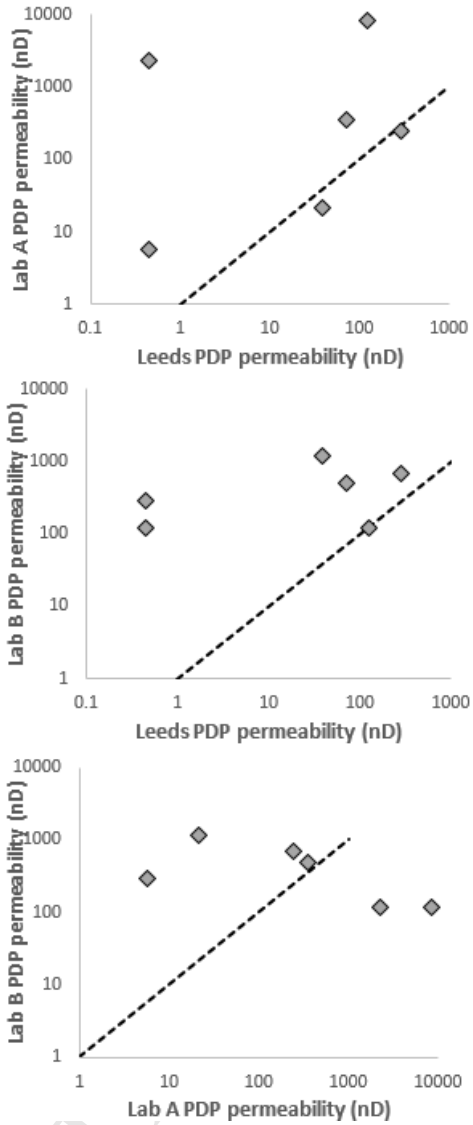

Figure 13 *Comparison of permeability values obtained from the crushed shale and core plug PDP technique.*

Discussion

Porosity

The results from the round-robin test conducted during the current study show far more agreement between the various laboratories than suggested by Passey et al. (2010). All laboratories provided very similar results for bulk density. Leeds, LabA and LabC produced very similar results for grain density (average stdev = 0.015g/cm^3) and porosity (stdev = 0.3 p.u.). This precision is quite similar to the accuracy that API suggest is typical for measurements conducted on conventional sandstones. The largest discrepancy between laboratories was between the grain densities and hence porosities obtained by LabB and the other laboratories. Handwerger et al. (2011) suggested that the reason for this discrepancy could reflect the method used to clean the samples and obtain oil and water saturations. In particular, Handwerger et al. (2011) argued that the Dean Stark method used by LabA

removes structurally bound water from clays and therefore results in higher porosities and grain densities. However, neither Leeds nor LabC cleaned the samples using this method and produced very similar grain densities to LabA. There is also no correlation between the difference in grain densities measured by LabB compared to the other laboratories and the clay content of the samples. This suggests that removal of structurally bound water from clay is not the reason that LabB produced lower porosities. Instead, the results are consistent with the interpretation of Lalanne et al. (2014) that LabB do not leave samples for a sufficient length of time within the retort apparatus to remove capillary bound water.

The similarity in results between Leeds, LabA and LabC is encouraging but it should not be used as evidence that these values accurately reflect subsurface porosity values. It is well know that the petrophysical properties of tight rocks are very stress dependent and there is a considerable amount of evidence that the properties of shale are equally if not more stress dependent particularly considering the damage that is often done to samples during coring and core retrieval (e.g. Heller et al., 2014). Indeed, microstructural analysis has shown that all samples contain microfractures that are very unlikely to exist in the subsurface (**Figure 14**). A method therefore needs developing to overburden correct bulk density and hence porosity values. It is relatively straight forward to conduct pore volume compressibility experiments on samples from conventional reservoirs in which the volume of brine expelled from the sample is measured as the confining pressure is increased. These experiments are often difficult to conduct on shale samples due to the difficulty of drilling and then saturating core plugs.

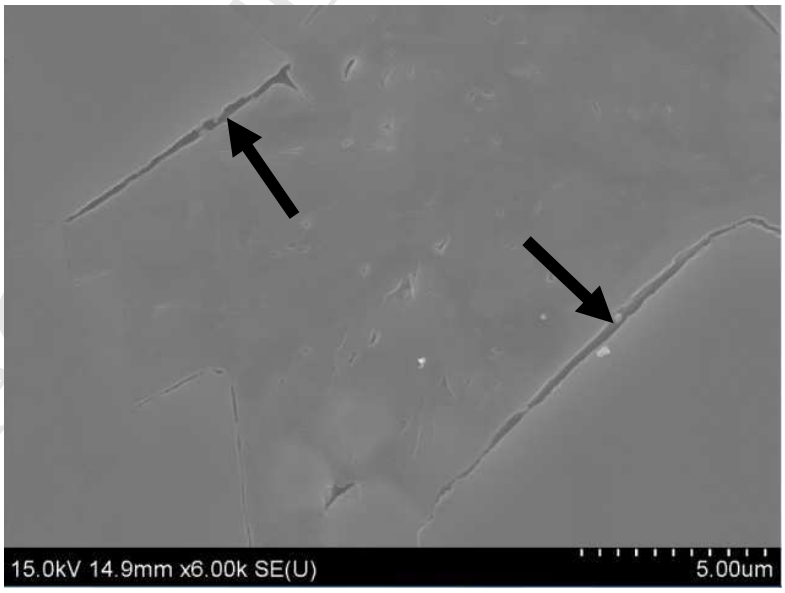

Figure 14 *SEM images showing stress release microfractures (arrows) in a shale sample.*

Permeability

Causes for differences between laboratories

The lack of correlation between the permeability measurements supplied by the different laboratories using the CSM is consistent with the round-robin test reported by Passey et al. (2010). Overall, the permeability values obtained by Leeds were several orders of magnitude lower than those provided by the commercial laboratories. Peng and Loucks (2016) reinterpreted pressure transient data from a turn-key CSM instrument supplied by one of the service companies. Their calculations produced permeabilities that were two orders of magnitude lower than the value produced by the instrument. We have also analysed the same raw data using the analytical and numerical methods described above and get very similar results to Peng and Loucks (2016). These results suggest perhaps that the results from one of the commercial laboratories could be in error due to issues related to the way in which permeability is calculated.

LabB did not provide enough details to allow us to identify the reason why their permeability values are far higher than the ones calculated by Leeds. LabC used the entire size range of <1/8 inch for their crushed shale permeability analysis. Peng and Loucks (2016) have indicated that there is a scale-dependence on shale permeability such that large samples have higher permeabilities. Alternatively, it is possible that the higher permeability values when using larger shale fragments is due to the assumption made regarding the lack of fractures within the shale particles. For example, Cui et al. (2009) presented data showing that increasing the size fraction used in the CSM resulted in higher permeability values (**Figure 15**). These permeability calculations assumed that the size of the shale particles was equal to their measured value. However, SEM analysis shows that crushed shale particles always contain a large density of microfractures (**Figure 16**). These microfractures could not exist under the effective stress conditions found in the subsurface and are likely to have formed either as a result of gas expansion during core retrieval or during the crushing process. These microfractures would allow easy access of the helium to the matrix porosity, which would invalidate the assumptions regarding the size of the particles used in algorithms to calculate permeability from pressure transient data. An end-member situation would be that crushed shale particles contain so many fractures that their effective particle-size is the same for the different size fractions and therefore each size fraction would produce the same pressure transient due to rapid helium flow along the fractures. To test the impact that this would have on the interpretation of pressure transient tests, an Eclipse^{TM} simulation has been run assuming that the sample has the same particle-size and permeability as the smallest particle-size shown for sample SH-12 in **Figure 15** (i.e. 0.4mm and 2.1 nD). The

pressure transient obtained from this simulation has then been used to calculate permeability assuming it was generated by experiments conducted with four other particle-sizes (0.8 mm, 1.6 mm, 3.2 mm and 6.4 mm). The results (**Figure 15**) have a remarkably similar slope to that of the data presented by Cui et al. (2009) and reflect the fact that if the same pressure transient is interpreted assuming different particle-sizes the calculated permeability will by necessity increase by the square of the assumed particle size divided by the particle-size used to calculate the pressure transient In other words, the higher permeabilities provided by the service companies could be due to the use of larger particles for the CSM analysis and the assumption that the individual shale particles do not contain fractures. However, another interpretation would be that the matrix permeabilities are actually far lower than calculated by the service companies but that the shale particles contain fractures (**Figure 15**).

Potentially one of the most striking observations regarding the results produced from the CSM is that they appear inconsistent with microstructural observations. In particular, we have access to a large amount of microstructural and petrophysical property data from tight gas sandstones that have permeabilities of <0.001 mD. Comparison of the microstructure of sample SH-3 (**Figure 17**), which the core analysis companies have determined has a permeability of 0.0001 to 0.001 mD with a tight gas sandstone with a similar permeability (**Figure 18**) indicate that the latter have pore sizes that are at least an order of magnitude larger than shale. These microstructural results are consistent with Hg-injection data (**Figure 19**) indicating that a shale sample has far smaller pore throats than a tight gas sandstone sample with similar measured permeability. Overall, it seems likely that this inconsistency is due to the inability of the CSM to produce reliable and accurate permeability results.

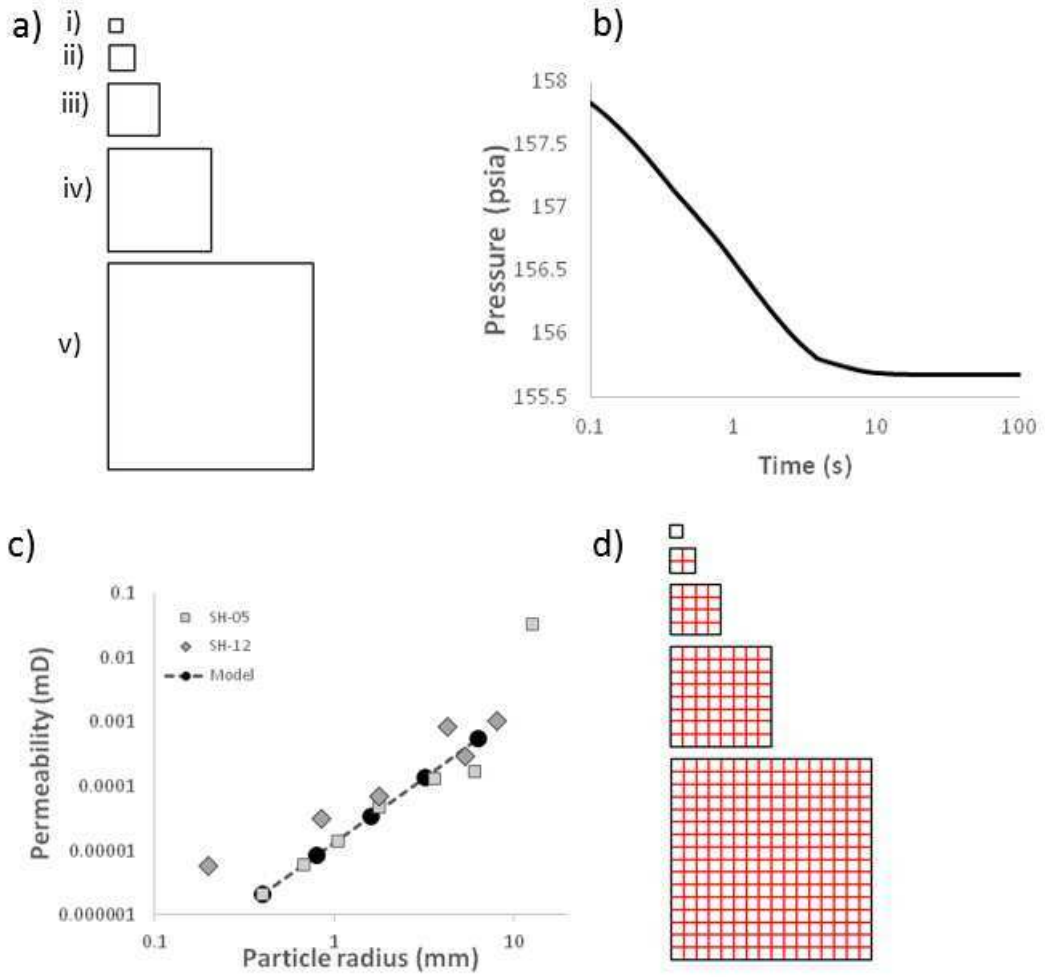

Figure 15 *Diagram to illustrate how the interpretation of CSM results is model dependent. If the same pressure transient shown in a) is produced from five different shale fractions with particle sizes represented by b) (with a minimum particle radius of 0.4 mm and largest of 6.4 mm) the calculated permeability will have a relationship with particle size as shown by the "model" results in c). However, if the particles are full of fractures with the same spacing as the minimum particle size as shown by the red lines in d) then the same pressure transient would be produced as shown in a) by all particles having the same matrix permeability as the smallest particle. The relationship between permeability and particle size is similar for the different size fractions of two crushed shale samples (SH-05, SH-12) presented by Cui et al. (2009). In other words, the relationship between fracture permeability and particle radius identified by Cui et al. (2009) is based on the assumption that individual shale particles do not contain fractures.*

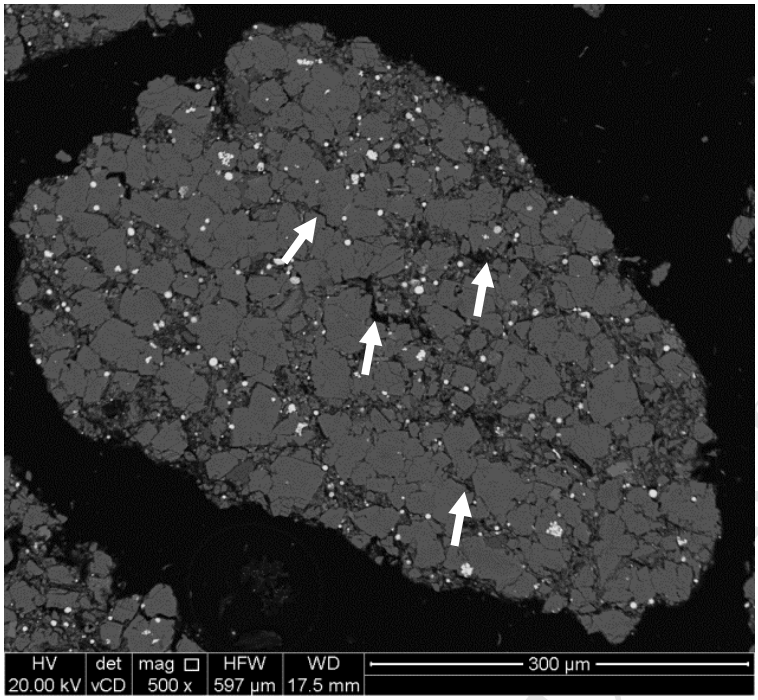

Figure 16 *BSEM micrograph of a crushed shale fragment; note the large number of microfractures present (e.g. white arrows).*

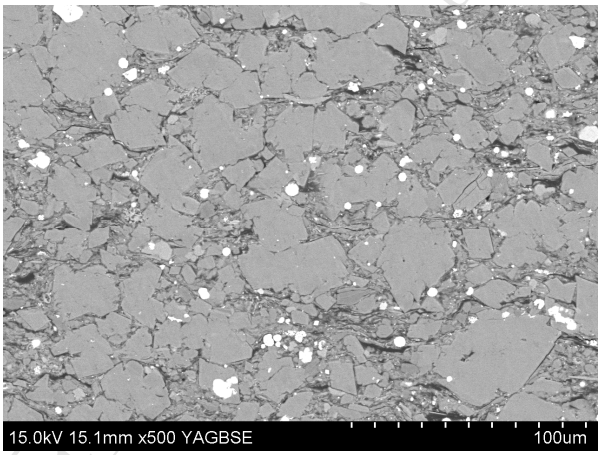

Figure 17 *Photomicrograph of sample SH3, for which the crushed shale analysis conducted by the service companies indicates that it has a permeability of 0.001 to 0.0001 mD. At this scale, pores are too small to be observed.*

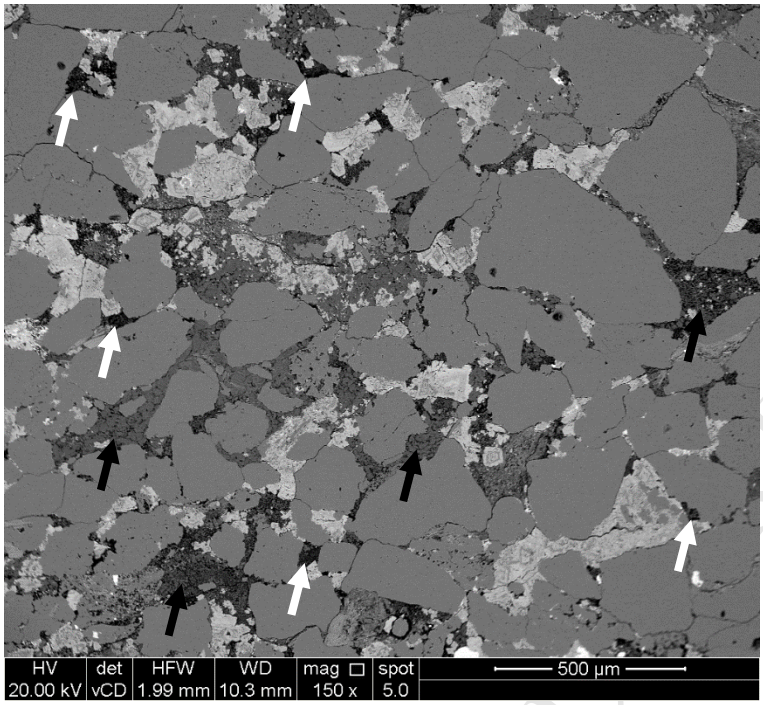

Figure 18 *Photomicrograph of sample a tight gas sandstone which has a gas permeability of 0.00085 mD. Note the difference in scale to the sample shown in* ***Figure 17*** *and the fact that macropores (white arrows); and micropores between kaolin platelets (black arrows) can be observed.*

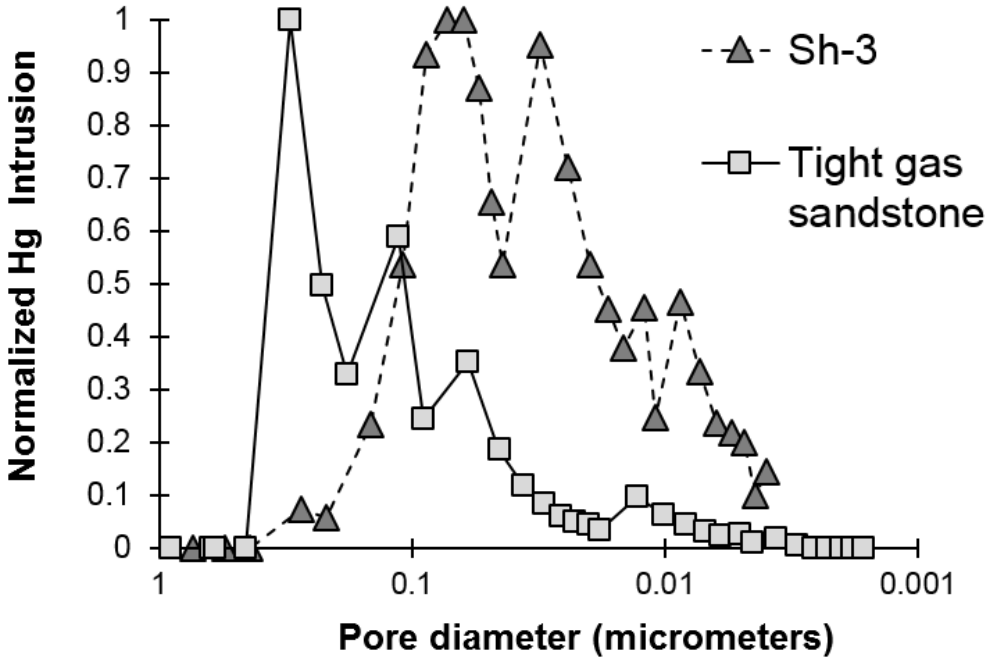

Figure 19 *Hg injection data from SH-3 and a tight gas sandstone with a gas permeability of 0.00085 mD.*

Implications of rapid gas entry into shale fragments

The original GRI report suggested it may be possible extrapolation the pressure vs time data to $t = 0$ and then apply Boyle's Law to calculate the shale volume within the sample chamber

(Luffel, 1993). Calculations conducted during this study suggest that the theoretical p_{i0} based on the weight of the shale fragments and their bulk density is significantly higher than the pressure estimated by extrapolating pressure to $t^{0.5} = 0$. The likely reason for this is that a significant amount of gas has entered the particles very soon (i.e. <1 s) after the valve connecting the sample chamber to the reference chamber is opened. The results obtained during this study cannot be used with certainty to identify the type of pore space into which this gas flows. It is possible that this pore space was created as a result of damage during coring, core retrieval or during sample preparation; such porosity has no relevance to subsurface performance and should be ignored. It is, however, possible that such pore space represents natural fracture and matrix porosity, which would be present in the subsurface. Such porosity would be incredibly important to characterize because it may be providing the highest permeability pathways in the subsurface. However, it is clear that the CSM cannot be used to measure the permeability of such pathways as they become filled with gas before temperature equilibrium has been reached within the sample chamber.

Eclipse™ simulations were also run to assess the sensitivity of the crushed shale method to key parameters such as sample permeability. For this sensitivity test, a series of models were run in which the permeability of the sample was varied between 100nD and 10 pD (10^{-12} D) and for porosities of 1% and 10%, as well as for particle sizes of 600 µm and 6 mm. A model was also run in which 17 layers had a permeability of 0.1 nD and one layer had a permeability of 100 nD. **Figure 20** shows results from simulated crushed shale experiments on rocks with 0.01 nD to 100 nD. A key observation is that pressure equilibration is extremely fast (<10 seconds) for samples with a permeability of >10 nD. The first few seconds of data obtained during these experiments are unreliable, which essentially means that the experiment is not suitable for analyzing samples with such high permeabilities. A model was also run containing a thin high permeability zone (could be sedimentary heterogeneity or fracture) in a 0.1 nD matrix. The results indicate that it would be almost impossible to identify this high permeability streak from the crushed shale test (**Figure 21**). Such higher permeability heterogeneities are likely to control the flow behavior of caprocks (and shale gas resource plays) but would not be identified using the crushed shale method.

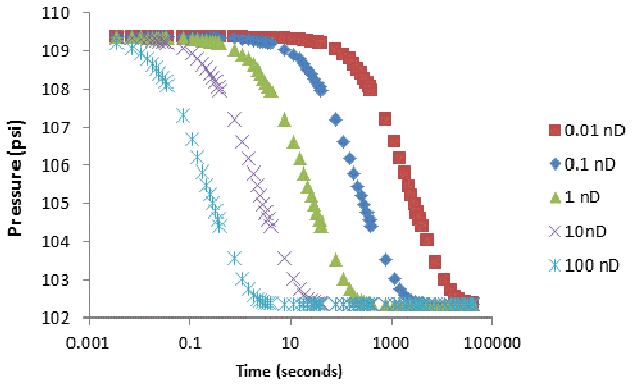

Figure 20 *Plots of the pressure decay vs time for simulated crushed shale experiments. The shale is assumed to have a porosity of 10%, a particle size of 600 µm x 600 µm x 1800 µm and permeabilities between 0.01 nD and 100 nD. Note that the equilibration is reached extremely quickly (<10 seconds) for particles with a permeability of 100 and 10 nD.*

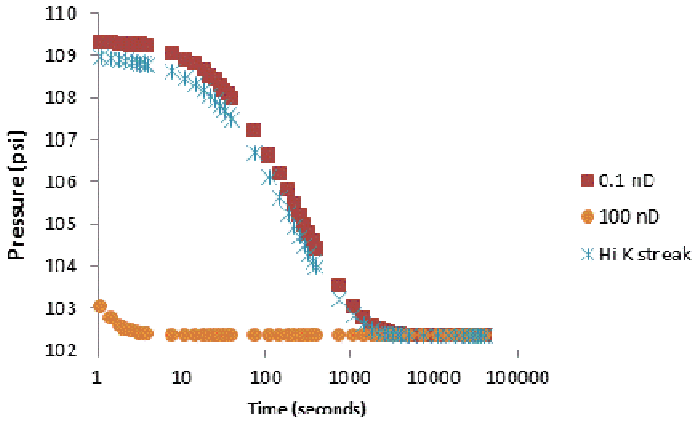

Figure 21 *Plots of the pressure decay vs time for simulated crushed shale experiments. The shale is assumed to have a porosity of 10%, a particle size of 600 µm x 600 µm x 1800 µm. Results from three models are shown. Two have homogenous permeabilities of 0.1 and 100nD. The third is composed of 0.1 nD shale with a 100 nD high permeability streak making up 5% of the pore volume.*

Recommendations for the use of the crushed shale method

The work conducted during the current study has highlighted several key problems when attempting to use the CSM to estimate the permeability of shale. A huge difference between the values provided by different laboratories (i.e. up to four orders of magnitude) suggests that results obtained from different laboratories cannot be compared even on a qualitative basis. Production simulation modelling is not commonly applied to shale gas plays so having accurate knowledge of subsurface permeability is probably not a major barrier to shale gas development. A precise measurement that reflected the gas flow potential of shale may, however, be useful for identifying producing analogues for shale resource plays undergoing appraisal. In particular, identification of suitable analogues may provide an early indication as to whether or not the shale under appraisal is likely to produce at economic rates. The lack of a standard approach between different laboratories in terms of the experimental

methodology or calculation of permeability from the pressure transient means that currently it is not possible to compare results obtained from different laboratories. However, even if methods were standardized, the crushed shale method would still have the problem that it does not seem sensitive to the presence of higher permeability streaks that may dominate flow in the subsurface. The results from the study therefore seem to indicate that the method is probably totally unsuitable for assessing the permeability of shale on either a quantitative or comparative basis.

There was, however, reasonable agreement between the laboratories regarding the porosity values generated using the crushed shale method. This agreement would be even further improved if a standard procedure was agreed upon to clean the crushed shale. There still, however, exists the problem of overburden correcting the porosity values. The difficulty in taking core plugs often means that it is difficult to obtain pore volume compressibilities using traditional methods. New methods therefore need to be developed to measure pore volume compressibilities on shale samples with uneven shapes. One possibility would be to use Hg injection analysis to assess the impact of stress on bulk volume. In particular, Hildenbrand and Urai (2003) presented evidence that Hg often does not actually enter the pore space of shale during Hg-injection experiments. If that was the case, the pressure vs injected volume curves obtained from Hg-injection experiments would in fact represent stress vs compressibility curves and could therefore be used to estimate the stress dependency of pore volumes. This clearly requires further work, however, the pore volume multipliers obtained from Hg injection experiments are very consistent with what would be expected from shale samples (i.e. 0.75 to 0.95). We are currently working on a technique to coat shale samples in a thin material that would totally prevent Hg entering pore space during Hg-injection experiments and then such results could be related to the compressibility of shale with more certainty.

Conclusions

The crushed shale method has been widely used by industry to measure the porosity and permeability of shale. Theoretically, the method offers many advantages over traditional laboratory techniques. The current study has conducted experimental measurements, numerical modelling and sent six samples to leading service companies for a round-robin test. The results suggest that the CSM test can provide precise estimates of porosity measured at ambient stress if standard sample cleaning techniques are used. There are, however, uncertainties regarding how overburden corrections are made. However, the results suggest that the CSM does not appear to be useful for measuring permeability in

either a quantitative or qualitative manner. It would probably be possible to make measurements more reproducible by adopting standard analytical methods across industry. However, even with standard workflows, the test may not be particularly useful as a guide to the flow capacity of shale because it is generally insensitive to the presence of high permeability streaks that may control subsurface gas flow.

Acknowledgements

We are extremely grateful for the sponsorship of this work provided by Chevron, EBN and Nexen. Schlumberger and Emerson are thanked for granting us licences to use Eclipse™ and Enable™.

Nomenclature

b Klinkenberg coefficient (Pa)

DV dead volume (m^3)

F_R mass fraction of gas

k apparent gas permeability $k = k_1(1+b/P)$ (m^2)

k_1 intrinsic permeability (m^2, D)

K term defined by $K = \frac{k}{\phi\mu\beta_f}$ (Equation 6)

K_c ratio of the dead volume in the experimental apparatus divided by the pore volume of the shale

m number of roots used in Equation (7)

P_{0i} initial pressure pulse (Pa)

$P_0(t)$ pressure at $r = R_0$ and t (Pa, psig, bar)

P_{1i} initial steady-state pressure (Pa, psig)

P_i pressure in the sample cell after the valve has been opened (Pa, psig)

P_f final steady state pressure (Pa, psig)

P_m mean value of P_0 over t_f (Pa)

r radial coordinate (m)

R_0 particles radius (m)

S_T particles total exchange area (m^2)

t time (s)

t_D dimensionless time

t_i date of measurement (s)

t_f duration of the experiment (s)

V_s sample cell volume (m^3)

V_0 reference cell volume (m^3)

V_1 crushed sample volume (m^3)

W_w weight of wet, crushed rock sample (g)

α_1 first root of the equation (11)

β_f ideal gas compressibility (Pa^{-1})

γ term defined by Equation (4)

δ term defined by Equation (5)

ϕ porosity, fraction

ξ_m roots of Equation (7)

ρ_b bulk density, g/cm^3

ρ_g grain density, g/cm^3

ρ_{c0} initial average gas density in the sample and reference cells

ρ_{r0} initial gas density in the reference cell

References

Ashena, R., Thonhauser, G., Vortisch, W., Prohaska, M., and Arabjamaloei, R. (2016) Geomechanical Simulation of Core Microfractures While Pulling Out Of Hole. International Symposium of the Society of Core Analysts, Snowmass, Colorado, Paper No SCA2016-091.

Brace, W.F., Walsh, J.B., Frangos, W.T. (1968) Permeability of Granite under High Pressure. J. Geophys. Res. 73 (6), 2225–2236.

Civan, F., Rai, C.S., Sondergeld, C.H. (2011a) Shale-Gas Permeability and Diffusivity Inferred by Improved Formulation of Relevant Retention and Transport Mechanisms. Transport in Porous Media 86 (3), pp. 925-944.

Civan, F., Rai, C.S., Sondergeld, C.H. (2011b) Shale Permeability Determined by Simultaneous Analysis of Multiple Pressure-Pulse Measurements Obtained under Different Conditions. Paper 144253-MS, Society of Petroleum Engineers. Paper presented at the North American Unconventional Gas Conference and Exhibition, 14-16 June, The Woodlands, Texas, USA.

Civan, F. and Devegowda, D. (2015) Comparison of Shale Permeability to Gas Determined by Pressure-Pulse Transmission Testing of Core Plugs and Crushed Samples. Paper SPE-178571-MS, Society of Petroleum Engineers. Paper presented at the Unconventional Resources Technology Conference held in San Antonio, Texas, USA, 20–22 July 2015.

Civan, F., Devegowda, D., Sigal, R. (2013) Critical Evaluation and Improvement of Methods for Determination of Matrix Permeability of Shale. Paper presented at the SPE Annual Technical Conference and Exhibition held in New Orleans, Louisiana, USA, 30 September–2 October 2013.

Cui, X., Bustin, A. M., Bustin, R. M. (2009) Measurements of Gas Permeability and Diffusivity of Tight Reservoir Rocks: Different Approaches and Their Applications: Geofluids, Vol. 9, pp. 208–223, doi: 10.1111/j.1468-8123.2009.00244.x.Curtis, M.E, Cardott, B.J., Sondergeld, C.H., and Rai, C.S. (2012) Development of organic porosity in the Woodford Shale with increasing thermal maturity. International Journal of Coal Geology, 103, 26–31.

Dadmohammadi, Y., Misra, S., Sondergeld, C.H. and Rai, C.S. (2016) Simultaneous Estimation of Intrinsic Permeability, Effective Porosity, Pore Volume Compressibility, and Klinkenberg-Slip Facture of Ultra-Tight Rock Samples Based on Laboratory Pressure-Step Decay Method. SPE 180266-MS

Dicker, A.I., Smits, R.M. (1988) A Practical Approach for Determining Permeability From Laboratory Pressure-Pulse Decay Measurements. Paper 17578-MS, Society of Petroleum Engineers. Paper presented at the International Meeting on Petroleum Engineering, 1-4 November, Tianjin, China.

Fischer G.J. and Paterson M.S. (1992) Measurement of permeability and storage capacity in rocks during deformation at high temperature and pressure. Fault Mechanics and Transport Properties of Rocks (51), pp. 213–252.

Freeman, C. M., Moridis, G. J., Blasingame, T. A. (2011) A Numerical Study of Microscale Flow Behavior in Tight Gas and Shale Gas Reservoir Systems. Transport Porous Media, 90: 253. doi:10.1007/s11242-011-9761-6

Handwerger, D. A., Suarez-Rivera, R., Vaughn, K. I. and Keller, J. F. (2011) Improved Petrophysical Core Measurements on Tight Shale Reservoirs Using Retort and Crushed

Samples. Paper 147456, Society of Petroleum Engineers. Paper presented at the Annual Technical Conference and Exhibition, Denver, USA, 30 October–2 November.

Haskett, W.J. (2014) The Myth of Sweet Spot Exploration. Paper SPE-170960-MS, Society of Petroleum Engineers. Paper presented at the SPE Annual Technical Conference and Exhibition, Amsterdam, The Netherlands, 27-29 October 2014.

Heller, R., Vermylen, J., Zoback, M. (2014) Experimental investigation of matrix permeability of gas shales. AAPG Bulletin, Vol. 98, No. 5, pp. 975–995.

Hildenbrand, A. and Urai, J.L. (2003) Investigation of the morphology of pore space in mudstones–first results. Marine and Petroleum Geology, Vol. 20, pp. 1185–1200.

Hsieh, P.A., Tracy, J.V., Neuzil, C.E., Bredehoeft, J.D., Silliman, S.E. (1981) A Transient Laboratory Method for Determining the Hydraulic Properties of 'Tight' Rocks–I. Theory. International Journal of Rock Mechanics and Mining Sciences and Geomechanics Abstracts 18 (3), pp. 245–252.

Hughes, J.D. (2015) Shale Gas Reality Check- Revisiting the U.S. Department of Energy Play-by-Play Forecasts through 2040 from Annual Energy Outlook 2015. Post Carbon Institute, California, USA.

IEA (2015) International Energy Agency. Online, available from: https://www.iea.org/

Javadpour, F. (2009) Nanopores and Apparent Permeability of Gas Flow in Mudrocks (shales and siltstone). J. Can. Pet. Technol. 48 (8), 16–21.

Jenkins, R. E. (1960) Accuracy of Porosity Determinations. Paper SPWLA-1960-E, Society of Petrophysicists and Well-Log Analysts. Paper presented at the First Annual Meeting of the Society of Professional Well Log Analysts, May 16-17, Tulsa, Oklahoma.

Jones, S. C. (1997) A technique for faster pulse-decay permeability measurements in tight rocks. Society of Petroleum Engineers, Paper SPE 28450.

Lalanne, B., Le-Binan, A., Elias, R., Poyol, E. and Martinez, L. (2014) Hope to cope with some of the challenges associated with laboratory measurements on gas shale core samples. Paper SPE 167709, Society of Petroleum Engineers.

Lin, W. (1977) Compressible Fluid Flow Through Rocks of Variable Permeability. Rep. UCRL -52304, 15 Lawrence Livermore Lab., Livermore, California.

Lorinczi, P., Burns, A.D., Lesnic, D., Fisher, Q.J., Crook, A.J., Grattoni, C. and Rybalcenko, K. (2014) Direct and Inverse Methods for Determining Gas Flow Properties of Shale. Paper SPE 167750, Society of Petroleum Engineers. Paper presented at the SPE/EAGE European Unconventional Conference and Exhibition held Vienna, Austria, 25–27 February 2010.

Luffel, D.L. and Guidry, F.K. (1992) New Core Analysis Methods for Measuring Rock Properties of Devonian Shale. Paper SPE-20571-PA, Society of Petroleum Engineers. Journal of Petroleum Technology, Vol. 44 (11), pp. 1184-1190.

Luffel, D.L., Guidry, K., Curtis, J.B. (1992) Evaluation of Devonian Shale with New Core and Log Analysis Methods. Paper SPE-21297-PA, Society of Petroleum Engineers. Journal of Petroleum Technology, Vol. 44 (11), pp. 1192-1197.

Luffel, D.L., Hopkins, C.W., Schettler Jr., P.D. (1993) Matrix Permeability Measurement of Gas Productive Shales. Paper 26633-MS, Society of Petroleum Engineers. Paper presented at the SPE Annual Technical Conference and Exhibition, 3-6 October, Houston, Texas.

Luffel, D.L. (1993) Advances in shale core analysis. Gas Research Institute, GRI Contract No 5086-213-1390.Neuzil, C.E., Cooley, C., Silliman, S.E., Bredehoeft, J.D., Hsieh, P.A. (1981) A Transient Laboratory Method for Determining the Hydraulic Properties of 'Tight' Rocks–II. Application. Int. J. Rock Mech. Min. Sci. Geomech. Abstr. 18 (3), pp. 253–258.

Mathur, A., Sondergeld, C.H., and Rai, C.S. (2016) Comparison of Steady-State and Transient Methods for Measuring Shale Permeability. Paper SPE 180259 – MS, Society of Petroleum Engineers.

Neuzil, C.E., Cooley, C., Silliman, S.E., Bredehoeft, J.D., Hsieh, P.A. (1981) A Transient Laboratory Method for Determining the Hydraulic Properties of 'Tight' Rocks–II. Application. Int. J. Rock Mech. Min. Sci. Geomech. Abstr. 18 (3), pp. 253–258.

Passey, Q.R., Bohacs, K., Esch, W.L., Klimentidis, R., Sinha, S. (2010) From Oil-Prone Source Rock to Gas-Producing Shale Reservoir - Geologic and Petrophysical Characterization of Unconventional Shale Gas Reservoirs. Paper SPE-131350-MS, Society of Petroleum Engineers. Paper presented at the CPS/SPE International Oil & Gas Conference and Exhibition in China held in Beijing, China, 8–10 June 2010.

Peng, S. and Loucks, B. (2016) Permeability measurements in mudstones using gas expansion methods on plug and crushed-rock samples. Marine and Petroleum Geology, 73, 299-310.

Profice, S., Lasseux, D., Jannot, Y., Jebara, N., Hamon, G. (2011) Permeability, Porosity and Klinkenberg Coefficient Determination on Crushed Porous Media. International Symposium of the Society of Core Analysts held in Austin, Texas, USA 18-21 September, 2011, Paper SCA2011-32.

Profice, S., Lasseux, D., Jannot, Y., Jebara, N., Hamon, G. (2012) Permeability, Porosity and Klinkenberg Coefficient Determination on Crushed Porous Media. Petrophysics, Vol. 53, No. 6, pp. 430–438.

Profice, S. (2014) Mesure de propriétés monophasiques de milieux poreux peu perméables par voie instationnaire. Applied Geology. Université de Bordeaux (French).

Tinni, A., Ebrahim Fathi, E., Agarwal, R., Sondergeld, C.H., Akkutlu, Y., Rai, C. (2012) Shale Permeability Measurements on Plugs and Crushed Samples. SPE-162235.Schieber, J. (2010) Common themes in the formation and preservation of intrinsic porosity in shales and mudstones – illustrated with examples across the Phanerozoic. Society of Petroleum Engineers, Paper SPE 132370.

Zubizarreta, I., Byrne, M., Jimenez, M.A., Rojas, E., Sorrentin, Y. and Velazco, M.A. **(**2011) Core Pressure Evolution and Core Damage: A Computational Fluid Dynamics Approach, Society of Core Analysts, *International Symposium of the Society of Core Analysts, Austin, Texas, Paper No* ***SCA2011-41.***

Zubizarreta, I., Byrne, M., Sorrentino, Y., Rojas, E. (2013) Pore Pressure Evolution, Core Damage and Tripping Out Schedules: A Computational Fluid Dynamics Approach, Society of Petroleum Engineers, Paper SPE-163527-MS.

Laboratory characterization of the porosity and permeability of gas shales using the crushed shale method: Insights from experiments and numerical modelling

Quentin Fisher, Piroska Lorinczi, Carlos Grattoni, Konstantin Rybalcenko, Anthony J. Crook, Samuel Allshorn, Alan D. Burns and Ida Shafagh

Highlights

- A round-robin test is reported where 6 shales were analyzed by 4 laboratories.
- Permeabilities measured by each laboratory using the crushed shale method (CSM) do not correlate.
- Permeabilities vary by orders of magnitude depending on how the data are interpreted.
- Results from the CSM method do not correlate with measurements made on core plugs.
- Pressure transient results from CSM experiments were inverted using analytical and numerical models.